Cardiovascular Innovations and Applications

Vol. 2 No. 1 (2017) 111–123
ISSN 2009-8618
DOI 10.15212/CVIA.2016.0063

REVIEW

Novel Approaches for the Use of Cardiac/ Coronary Computed Tomography Angiography

Hadi Mirhedayati Roudsari, MD[1,a], Donghee Han, MD[1,a], Bríain ó Hartaigh, PhD[1], Ji Hyun Lee, MD[1], Asim Rizvi, MD[1], Mahn-won Park, MD[1], Bin Lu, MD[2], Fay Y. Lin, MD[1], and James K. Min, MD[1]

[1]*Dalio Institute of Cardiovascular Imaging, Department of Radiology, New York-Presbyterian Hospital and Weill Cornell Medicine, New York, NY, United States*
[2]*State Key Laboratory of Cardiovascular Disease, Fuwai Hospital, Beijing, China*

Received: 13 December 2016; Revised: 14 February 2017; Accepted: 15 February 2017

Abstract

Recent developments in the novel imaging technology of cardiac computed tomography (CT) not only permit detailed assessment of cardiac anatomy but also provide insight into cardiovascular physiology. Foremost, coronary CT angiography (CCTA) enables direct noninvasive examination of both coronary artery stenoses and atherosclerotic plaque characteristics. Calculation of computational fluid dynamics by cardiac CT allows the noninvasive estimation of fractional flow reserve, which increases the diagnostic accuracy for detection of hemodynamically significant coronary artery disease. In addition, a combination of myocardial CT perfusion and CCTA can provide simultaneous anatomical and functional assessment of coronary artery disease. Finally, detailed anatomical evaluation of atrial, ventricular, and valvular anatomy provides diagnostic information and guidance for procedural planning, such as for transcatheter aortic valve replacement. The clinical applications of cardiac CT will be extended with the development of these novel modalities.

Keywords: Coronary computed tomography angiography; fractional flow reserve; computational fluid dynamics; coronary artery disease; myocardial computed tomography perfusion

Introduction

Recent developments in cardiac computed tomography (CT) have enabled reliable visualization of the coronary artery and noninvasive detection of coronary artery disease (CAD). Prior studies have focused on technology assessment for coronary artery stenosis evaluation, demonstrating a high diagnostic accuracy for obstructive CAD, and the safety of coronary CT angiography (CCTA) as an alternative noninvasive evaluation compared with stress testing [1–4]. Current guidelines recommend CCTA be performed for evaluation of CAD, especially for those patients who have a low-to-intermediate pretest likelihood of CAD [5, 6]. However, clinical use of CCTA to date has focused on evaluation of luminal stenosis, which is of limited value for identifying hemodynamically significant CAD [7]. In an effort to overcome these drawbacks, researchers have recently developed novel approaches to CCTA to estimate the hemodynamic significance of CAD and to evaluate extraluminal plaque for

[a]Hadi Mirhedayati Mirhedayati and Donghee Han contributed equally to this work.

Correspondence: James K. Min, MD, FACC, Dalio Institute of Cardiovascular Imaging, New York-Presbyterian Hospital and the Weill Cornell Medicine, 413 E. 69th Street, Suite 108, New York, NY 10021, USA,
Tel.: +1-646-9626192, E-mail: jkm2001@med.cornell.edu

prognostication of adverse cardiac outcomes. Additionally, cardiac CT images contain noncoronary, 3D structural information of the whole heart at high spatial resolution. We review here novel approaches of cardiac CT for evaluation of cardiovascular disease.

CCTA for Detection of Atherosclerotic Plaque Characteristics

Beyond the detection of coronary stenosis, CCTA has also been used to evaluate extraluminal atherosclerotic plaque characteristics. Calcification and its absence are easily visualized in CCTA images. Early studies of plaque characteristics were limited to classification of calcified, noncalcified, or mixed plaque (Figure 1, panels A–C). The accuracy of this simple qualitative plaque measurement approach showed that the corrected rate of categorization of calcified, noncalcified, and mixed plaque by CCTA was 83, 94, and 95% respectively, with use of intravascular ultrasonography (IVUS) as the gold standard [9, 10].

Vulnerable plaque characteristics that predict downstream events are difficult to examine in vivo except by invasive techniques [11]. Recently, increased spatial and temporal resolution of CCTA has allowed the assessment of vulnerable plaque characteristics by the CT attenuation pattern (Figure 1, panels D–F) [12–14]. First, lipid-rich plaques may be identified on CCTA as low-attenuation plaques (LAP). Choi et al. [15] reported that plaques with more than 10% necrotic core on IVUS had a significantly lower CT density as compared with plaques with less than 10% necrotic core (41.3 HU vs. 93.1 HU). Previous studies have attempted to determine a distinct HU cutoff for LAP. A CT density of less than 30 HU has typically been used as a cut off for identification of LAP [16]. Second, positive remodeling, which represents the tendency of the coronary artery to undergo a compensatory enlargement with development of atherosclerosis, can also be identified by CCTA. Achenbach et al. [17] demonstrated that measurements of the remodeling index (RI) by CCTA were verified by IVUS, revealing a significantly high correlation (r^2=0.82). The degree of positive remodeling is typically overestimated by CCTA. When RIs were compared for thresholds of 1.05 and 1.1, RI of 1.1 in CCTA better identified positively remodeled plaque in IVUS with a sensitivity of 83% and a specificity of 78% as compared with the standard cutoff of RI of 1.05 (sensitivity 83% vs. 100% respectively; specificity 78% vs. 45% respectively) [18]. Third, the napkin-ring sign is a specific attenuation pattern of atherosclerotic plaques on CCTA images characterized by a plaque core with low CT attenuation surrounded by a rim-like area of higher CT attenuation (Figure 1, panel F), which may potentially represent thin-cap fibroatheroma. Kashiwagi et al. [19] demonstrated that the sensitivity, specificity, positive predictive value, and negative predictive value of the napkin-ring sign for detection of thin-cap fibroatheroma on optical coherence tomography are 44, 96, 79, and 85% respectively. Lastly, spotty calcification, which has been defined as distinct calcifications 3 mm or less in length and circumscribing an arc of 90° or less in CCTA cross section, potentially represents microcalcification in histology studies. Spotty calcification has significant association with vulnerable plaque characteristics defined by virtual histology–IVUS [20]. However, "spotty calcification" on CCTA is actually macrocalcification due to the limitation of the spatial resolution of current-generation CT scanners. There are also conflicting results among previous studies about the relationship between spotty calcification and plaque rupture [21].

Vulnerable CCTA plaque characteristics are not only correlated to invasive imaging but also contribute an independent prognostic value for future adverse events. Motoyama et al. [22] reported that significantly higher rates of acute coronary syndrome occurred in patients with one-feature- and two-feature-positive plaque (i.e., positive remodeling and LAP) when compared with patients with no high-risk plaque characteristics (49 vs. 3.7 vs. 22.2% respectively, P<0.001). A positive remodeled segment with LAP on CCTA was at a higher risk of future acute coronary syndrome (hazard ratio 22.8, 95% confidence interval [CI] 6.9–75.2) [22]. In the latter study, only 0.5% of patients without either feature had an acute coronary event, providing a strong negative predictive value. In addition to positive remodeling and LAP, Otsuka et al. [23] reported that the napkin-ring sign demonstrated on CCTA was strongly associated with future acute

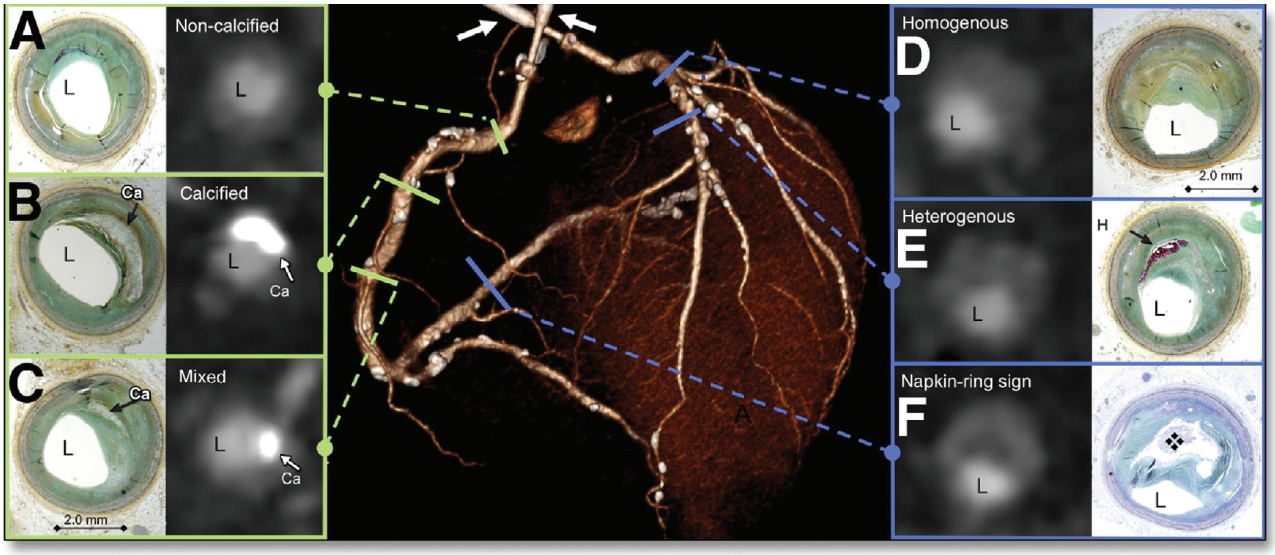

Figure 1 Traditional and Attenuation Pattern–Based Plaque Classification Schemes in Coronary Computed Tomography Angiography (CCTA).
The *center panel* shows a volume-rendered CCTA image of a cadaver heart. The traditional plaque classification scheme (left) differentiates between noncalcified plaques (A), calcified plaques (B), and partially calcified (mixed) plaques (C). The attenuation pattern–based classification scheme (right) differentiates between homogeneous plaques (D), heterogeneous plaques (E), and napkin-ring plaques (F). The corresponding histology slides show pathological intimal thickening (A), fibrous plaque with sheet calcification (B), pathological intimal thickening with spotty calcification (C), a fibrous plaque (D), early fibroatheroma with intraplaque hemorrhage (arrow) (E), and a late fibroatheroma with large necrotic core (E). Ca, calcium; L, lumen. Reproduced from Maurovich-Horvat et al. [8] with permission from Elsevier.

coronary syndrome events (hazard ratio 5.55, 95% CI 2.10–14.70), independent of other high-risk coronary CCTA features (e.g., positive remodeling and LAP). Furthermore, the Rule Out Myocardial Infarction/Ischemia Using Computer Assisted Tomography (ROMICAT) trial also demonstrated that high-risk plaque characteristics, including positive remodeling, LAP, napkin-ring sign, and spotty calcification, were significant predictors of myocardial infarction and unstable angina (odds ratio 8.9, 95% CI 1.8–43.3) [24]. A more recent study by Park et al. [25] reported that CT plaque characteristics were also associated with ischemic lesions as identified by invasive fractional flow reserve (FFR). In that study, the presence of positive remodeling and LAP displayed a fivefold and twofold increase respectively in the likelihood of significant ischemia.

Despite the potential applications of CCTA for identifying plaque characteristics, several studies using conventional single-energy CT have shown limited value for classification of the coronary artery plaque due to substantial density overlap between fibrous-rich and lipid-rich components [26, 27]. To resolve this limitation, dual-energy CT could potentially be applied to detect lipid-rich plaque, including necrotic core. The concept of dual-energy CT is simultaneous imaging with two energy spectra to differentiate between two materials with regard to their energy-specific attenuation profile [28, 29]. In a prospective study using 1,088 plaque areas co-registered by virtual histology–IVUS, Obaid et al. [30] showed a higher sensitivity (64%) and specificity (98%) for differentiation of necrotic core and fibrous plaque in ex vivo postmortem hearts in comparison with single-energy CT (sensitivity 50%, specificity 94%). Consideration of the application of dual-energy CT for identification of high-risk plaque characteristics is still in its infancy, and further studies of this concept are needed.

FFR Derived from CT

In the recent past, revascularization based on invasive FFR, the gold standard for determining the hemodynamic significance of coronary artery

lesions [31], has improved clinical outcomes [32]. FFR is defined as the ratio of the maximal flow in a stenotic artery to the hypothetical maximal flow in the same artery without stenosis [31]. Despite the clinical utility of invasive FFR, it is used in less than 10% of revascularization decisions, likely owing to the invasive nature, time-consuming approach, which is confined to the catheter laboratory, and the need for vasodilator medication [33]. The combination of CCTA with precise 3D anatomical imaging of the coronary artery anatomy, computational fluid dynamics, and image-based modeling allows estimation of FFR derived from CT (FFR-CT) to evaluate the hemodynamic significance of coronary lesions without additional radiation exposure and vasodilator injection [34, 35] (Figure 2). To date, several prospective, international multicenter studies have validated the diagnostic accuracy of FFR-CT as compared with invasive FFR as the reference standard. The Diagnosis of Ischemia-Causing Stenosis Obtained via Noninvasive Fractional Flow Reserve (DISCOVER-FLOW) study assessed the diagnostic performance of FFR-CT in 159 vessels in 103 patients using invasive FFR as the reference standard. In that investigation, the diagnostic accuracy of FFR-CT on a per-vessel basis was 84.3% (95% CI 77.7–90.0%) compared with 58.5% (95% CI 50.4–66.2%) for CCTA alone. Furthermore, a higher area under the curve was observed for FFR-CT when compared with CCTA on both a per-vessel basis (0.90 vs. 0.75, P=0.001) and a per-patient basis (0.92 vs. 0.70, P=0.0001) [36]. The Determination of Fractional Flow Reserve by Anatomic Computed Tomographic Angiography (DeFACTO) trial studied 252 patients, including 407 vessels, to determine the accuracy of FFR-CT compared with invasive FFR. In that study, a higher diagnostic accuracy was observed for FFR-CT for ischemia detection when compared with CCTA alone (73% [95% CI 67–78%] vs. 64% [95% CI 58–70%] respectively). Although the DeFACTO trial did not meet the prespecified primary end point for noninferiority, FFR-CT demonstrated an improved discriminatory power for ischemia as compared with CCTA alone in both a per-vessel basis (0.81 vs. 0.75, P<0.001) and a per-patient basis (0.81 vs. 0.68, P<0.001) [37]. The Analysis of Coronary Blood Flow Using CT Angiography: Next Steps (NXT) trial evaluated the diagnostic performance of FFR-CT in 254 patients, including 484 vessels, using invasive FFR as the reference standard. On a per-patient basis, the diagnostic accuracy (81%) and specificity (79%) for FFR-CT were markedly higher than the diagnostic accuracy (51%, P<0.0001) and specificity (32%, P<0.0001) for CCTA alone. The improved diagnostic accuracy compared with the diagnostic accuracy in DISCOVER-FLOW and DeFACTO is likely due to substantial refinement in FFR-CT technology, coronary modeling, and improved CT image quality [38].

In prior trials, FFR-CT calculation required off-site processing of CT datasets, which required hours of supercomputer calculations [34]. Improved software and hardware allows the availability of on-site workstation-based rapid post-processing of CCTA images. Several retrospective single-center trials have validated on-site methods in comparison with invasive FFR [39–41]. Among those studies, Coenen et al. [40] evaluated the diagnostic performance of on-site FFR-CT compared with CCTA using invasive FFR as the reference standard. On-site FFR-CT provided an incremental value over CCTA for detection of hemodynamically significant CAD (area under the curve 0.83 vs. 0.64). To evaluate the clinical outcomes of FFR-CT, the multicenter Prospective Longitudinal Trial of FFR-CT: Outcome and Resource Impacts (PLATFORM) [42] enrolled 584 patients with an intermediate likelihood of obstructive CAD and used two diagnostic strategies: usual care testing (n=287) or FFR-CT (n=297). The rate of invasive coronary angiography (ICA) displaying no obstructive CAD within 90 days as the primary end point was 73.3% in the planned ICA stratum versus 12.4% in the FFR-CT stratum (P<0.001). The authors concluded that FFR-CT significantly decreases the rate of unnecessary ICA as an invasive decision-making diagnostic tool [42]. Consequently, investigators evaluated the same cohort for 1-year outcomes of major adverse cardiac events, total medical costs, and quality of life [43]. A rare incidence of major adverse cardiac events was observed, including two events in the FFR-CT group and two events in the usual care group. The FFR-CT group demonstrated a significant lower medical cost as compared with the usual care group ($8,127 vs. $12,145; P<0.0001). In addition, the FFR-CT group had significantly

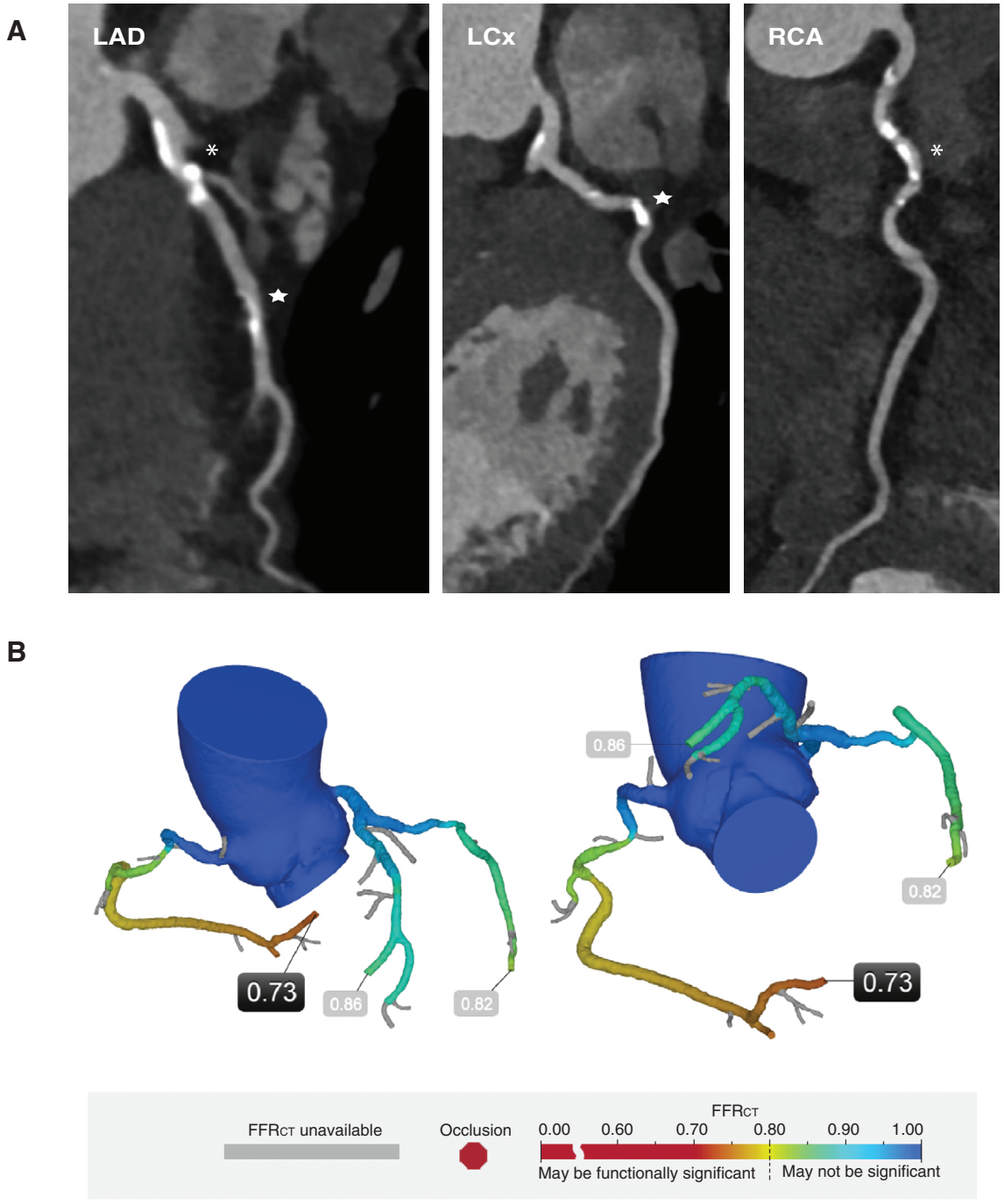

Figure 2 A 65-year-old White Man with Atypical Chest Pain.
(A) Multiplanar reformat of a computed tomography (CT) angiogram demonstrating a diffuse calcification in the proximal part of the left anterior descending coronary artery (LAD), a focal calcification in the middle part of the LAD, a focal calcification in the middle part of the left circumflex artery (LCx), and a diffuse calcification in the proximal part of the right coronary artery (RCA). (B) The fractional flow reserve derived from CT (FFRct) of the LAD, LCx, and RCA is 0.86, 0.82, and 0.73; the value for the RCA indicated significant ischemia. Lesions with diffuse and focal calcification in (A) are indicated by *asterisks* and *stars*.

increased quality-of-life scores versus the usual care group (mean change 0.12 vs. 0.07; P=0.02) [43].

The utility of FFR-CT for predicting poststenting outcomes using virtual stenting is a new and potentially useful application of this modality. Kim et al. [44] compared FFR-CT (before and after virtual stenting) with invasive FFR (before and after actual stenting) in 44 patients. The diagnostic accuracy of FFR-CT for forecasting ischemia

after stenting was 96% (sensitivity 100%, specificity 96%). Ongoing multicenter prospective trials such as the Computed Tomographic Evaluation of Atherosclerotic Determinants of Myocardial Ischemia (CREDENCE) [45], Dual Energy CT for Ischemia Determination Compared to "Gold Standard" Non-Invasive and Invasive Techniques (DECIDE-Gold) [46], and Computed Tomography Angiography in the Evaluation of Suspected Coronary Artery Disease (PERFECTION) [47] trials are comparing the diagnostic performance of FFR-CT versus other myocardial perfusion tests to determine which test is most applicable for use in the clinical setting. As further advancements are being made in CT technology with the goal of optimizing image quality and enhancing postprocessing software, FFR-CT is emerging as a safe, accurate, and cost-effective gatekeeper for ICA for the noninvasive evaluation of myocardial ischemia.

Myocardial CT Perfusion Analysis

Despite the high negative predictive value of CCTA for diagnosis of CAD, current applications of CCTA mainly provide only anatomical information on coronary artery stenosis [7, 48–50]. In addition, CCTA has limited accuracy to detect stenosis in vessels with dense calcification and in-stent restenosis [51, 52]. To overcome these shortcomings, increases in CCTA temporal resolution and increased detector row width have allowed the evaluation of myocardial CT perfusion (CTP) with CCTA for simultaneous anatomical and functional assessment of CAD in a single examination [53]. Moreover, the increased spatial resolution along with the shorter acquisition time makes it an appropriate choice compared with other conventional myocardial perfusion imaging methods, such as single photon emission CT [54, 55].

Numerous studies have assessed the diagnostic performance of myocardial CTP technologies. Bettencourt et al. [56] evaluated the diagnostic accuracy of CCTA and a myocardial stress-rest CTP combination using static single energy in patients with intermediate-to-high pretest probability of CAD as compared with quantitative coronary angiography. In a patient-based model, the accuracy of combined CCTA and CTP for detection of 50 and 70% stenosis was 84 and 93% respectively. They also reported a lower radiation dose required for the complete protocol as compared with other similar studies. In the Coronary Artery Evaluation Using 320-Row Multidetector Computed Tomography Angiography and Myocardial Perfusion (CORE320) study [57], a combination of stress-rest myocardial CTP and CCTA using a static CT scan decreased sensitivity, but substantially increased specificity and diagnostic accuracy of CCTA for identification of obstructive CAD. In a recent meta-analysis of myocardial CTP, the vessel-based sensitivity and specificity of combined CT angiography and single-phase stress CT for detection of 50% stenosis based on ICA were estimated to be 84 and 93% respectively [58].

Some inherent limitations of myocardial CTP include artifacts and radiation dose (Table 1). The main artifacts of CTP include beam hardening and motion artifacts. Use of prospectively ECG-triggered dual-energy CT along with some additional improvements in beam-hardening correction algorithms has, in part, solved these issues [59, 60]. Motion artifacts mostly occur as a consequence of elevated heart rate, and can be distinguished from true perfusion defects by use of some simple rules during image interpretation [61]. High radiation dose associated with CTP is still a major drawback, particularly in dynamic CT within a range of 5–13 mSv. The radiation dose range for static CT has been reported to be between 2 and 9 mSv in various studies [58]. A reduction in tube voltage and current together with use of iterative algorithms to enhance the image reconstructions can help decrease the radiation dose [62]. Kim et al. [63] demonstrated a reduction in radiation dose with preserved image quality using dynamic CT with 80 kV and a high-concentration iodine contrast agent. Nonetheless, to overcome some of the existing drawbacks of myocardial CTP, further studies are needed to determine the optimal protocol in tandem with advances in technology and postprocessing software to establish the lowest radiation dose.

Although the feasibility and high diagnostic performance of myocardial CTP are apparent, to date, there is no universal agreement for its indications, placement, and prognostic value in the prevention and treatment of cardiovascular diseases. Further still, it has remained a challenge to determine the optimal technology and protocol. Clearly, additional well-designed multicenter studies with sufficient power are required to determine the most

Table 1 Advantages and Disadvantages of Computed Tomography Perfusion Analysis.

	Advantages	Disadvantages
Resting CT perfusion	No need for additional radiation and drug administration	Low diagnostic accuracy to detect myocardial ischemia that is induced only in the stress phase Unable to distinguish reversible myocardial ischemia from irreversible myocardial ischemia
Stress CT perfusion	More accurate evaluation of reversible perfusion defect	Additional radiation dose Administration of medication to induce stress
Static CT	Lower radiation dose	Peak contrast attenuation may be missed More artifacts Low accuracy in multivessel defects
Dynamic CT	High temporal resolution Direct measurement of myocardial perfusion using fully quantitative assessment to measure absolute blood flow values	High radiation dose Respiratory motion artifacts due to long breath-hold (>30s) Spatial misalignment Cannot be used for assessment of coronary artery morphologic features

CT, computed tomography.

appropriate protocol, indications, and associated cost-benefit of this modality.

Other Applications of Noncoronary Cardiac CT

Cardiac Chamber Assessment

Given the high spatial resolution, anatomical assessment of extracoronary findings by means of cardiac CT can provide precise measurements of left ventricular morphology, such as chamber dimensions and volumes as well as left ventricular ejection fraction (LVEF). In a meta-analysis, the accuracy of cardiac CT scanning for LVEF measurement was compared with that of transthoracic echocardiography (TTE) and magnetic resonance imaging (MRI). Cardiac CT presented an accurate LVEF estimation when compared with MRI and TTE: the results of a meta-analysis showed that there are no significant differences in LVEF estimation between CT versus MRI and TTE (weighted mean difference between CT and MRI – 0.11 [95% CI – 1.48 to 1.26]; weighted mean difference between CT and TTE 0.19 [95% CI – 1.13 to 1.50]) [64]. However, because of the complex geometry, endocardial trabeculae, and enhancement problems, the associated accuracy of cardiac CT for volumetric assessment of the right side of the heart appears to be limited [65]. Moreover, in terms of limitations, premedication with beta-blockers before cardiac CT can diminish myocardial tone, which may lead to alterations in actual volumes and ejection fraction measurements. In addition, the assessment of cardiac chambers requires a retrospective protocol covering both systolic and diastolic phases, as compared with other procedures. Thus it is not feasible to apply a radiation dose–reducing strategy such as low-dose step and shoot protocols.

Assessment for Congenital Heart Disease

The rapid acquisition ability of CCTA enables precise evaluation of patients with congenital heart diseases (CHD), especially in children with fast cardiac rhythm [66]. While echocardiography is the primary diagnostic method for CHD for all ages, cardiac CT is used as a complementary tool especially for the assessment of extracardiac vessels and coronary arteries [67]. In addition, cardiac CT can be used for preoperative assessment as well as postoperative evaluation [68]. Current guidelines have several recommendations for the applications of cardiac CT in patients with CHD [69]. Coronary anomalies may affect the surgical plan in patients with CHD, and accurate anatomical assessment of coronary arteries by cardiac CT is recommended before surgery [70]. Additionally, the ability of cardiac CT to evaluate systemic and pulmonary

vessels as well as ventricular size and function allows preprocedural and postprocedural assessment in patients with aortic coarctation, pulmonary venous anomaly, tetralogy of Fallot, and transposition of great arteries [71–74]. Although cardiac CT is an excellent diagnostic method for CHD, it has limitations compared with echocardiography such as the need for sedation in young children, intravenous access for contrast agent injection, and risk of radiation exposure [69].

Periprocedural Assessment

Transcatheter aortic valve replacement (TAVR) is a newly developed procedure to treat patients with severe aortic stenosis with moderate to high surgical risk. Recent randomized controlled trials have reported that patients who underwent TAVR displayed improved long-term outcomes as compared with patients with inoperable aortic stenosis because of high surgical risk who received standard treatment [75, 76]. Before TAVR, evaluation of aortic valve and adjacent structure is essential to estimate the feasibility of TAVR and periprocedural complication risk. The aortic annulus is a complex noncircular and dynamic structure with continuous morphological changes throughout the cardiac cycle. Traditionally, echocardiography and invasive cardiac catheterization were used for preprocedural evaluation of TAVR; however, they provided limited data because of the nature of the 2D imaging technique and shadowing by calcification. Cardiac CT can overcome these limitations and improve patient and valve selection [77].

The sizing of the TAVR valve is an important step in procedural planning for TAVR. Cardiac CT has many advantages in addition to superior results with respect to TAVR valve sizing. Paravalvular aortic regurgitation (PAR) is a potentially important complication, and is closely related to TAVR valve size. More than mild PAR after TAVR is associated with a 2.5-fold increased risk of all-cause death when compared with no PAR [78]. When compared with transesophageal echocardiography (TEE) and invasive angiography-based TAVR valve sizing, CT-based aortic annular evaluation for TAVR valve sizing is associated with a 7–14% significant reduction in the incidence of post-TAVR PAR that is more than mild [79, 80]. Preevaluation of valve sizing using cardiac CT measurement has been shown to have higher reproducibility when compared with use of TEE [81].

Cardiac CT provides comprehensive information about the distance to coronary ostia and the presence of calcific nodules for appropriate patient selection. Measurement of the adequate height of the coronary ostia is an important prerequisite for the TAVR procedure. In a multicenter study from 81 centers, 44 of 6,688 patients had acute symptomatic coronary obstruction following the procedure [82]. Lower-lying coronary ostium (<12 mm) and shallow sinuses of Valsalva (<30 mm) were the strongest anatomical factors associated with coronary obstruction. Generally, ostia heights more than 12 mm from the annulus are considered safe for avoidance of coronary ostial obstruction. Aortic root injury or rupture is the other serious complication of the TAVR procedure. Cumulative left ventricular outflow tract (LVOT) and annulus rupture rates of 1.1 and 0.9% respectively have been reported [83, 84]. An advantage of cardiac CT for the prevention of aortic root injury is that the severity and location of calcification in the LVOT can be determined. In a multicenter registry, Hansson et al. [85] reported that the median calcium volume within the LVOT in patients found to have aortic root injury was 74 mm^3 compared with 3 mm^3 in patients without observed root injury.

Radiofrequency catheter ablation (RFCA) of the pulmonary veins (PV) has become a frequent interventional therapy for refractory atrial fibrillation. Cardiac CT can be useful to demonstrate individual 3D anatomical geometry of the left atrium (LA), left atrial appendage (LAA), and PV for procedural planning in atrial fibrillation before ablation. Three-dimensional electroanatomical mapping by cardiac CT can support the catheter ablation procedure for successful RFCA [86, 87]. Not only is it informative in defining anatomical characteristics, cardiac CT also enables the ruling out of the presence of LAA and LA thrombus in patients before they undergo electric cardioversion or ablation procedures. In cardiac CT images, LAA thrombus will appear as areas with hypoattenuation or haziness, but slow blood flow in the LAA could be a common cause of false positive results especially in early-phase images. For exclusion of "pseudothrombus," the addition of a noncontrast delayed image is useful in reducing the false positive rate. In a meta-analysis, the diagnostic

accuracy, sensitivity, specificity, positive predictive value, and negative predictive value of cardiac CT for detection of LA/LAA thrombi were 94, 96, 92, 41, and 99% respectively when compared with TEE as a reference standard [88]. Furthermore, a clinical integration of cardiac CT to assess the LAA before RFCA markedly reduced the number of TEE procedures and an showed excellent safety profile [89].

Cardiac CT is also important for other procedural planning and device evaluation. Although transcatheter mitral valve replacement is not yet widely clinically available, cardiac CT is promising for valve sizing and prevention of complications [90]. Lastly, 3D printing is expected to have a wide use in structural heart interventions soon. Given the high spatial resolution and 3D multiplanar reformatting capabilities, it is anticipated that cardiac CT will likely play a pivotal role in 3D printing device development and interventional planning [91].

Conclusion

At present, cardiac/coronary CT is commonly performed for obstructive CAD evaluation. Recent developments in CT technology, however, now enable us to extend the application of cardiac CT to the evaluation of coronary plaque characteristics that previously were considered assessable only by the use of invasive imaging modalities. In addition, myocardial CTP analysis and FFR-CT allow the evaluation of not only anatomical but also functional assessment of CAD by a single modality. The use of cardiac CT to evaluate extracoronary findings has resulted in this procedure being progressively used as an essential noninvasive imaging tool for the evaluation of cardiac structure and function and preprocedural evaluation. Future anticipated technical improvements related to CCTA, including dual-energy CT and 3D printing, may allow the development of new tools for improving patient care in cardiovascular disease.

Acknowledgments

This work was supported by a generous gift from the Dalio Institute of Cardiovascular Imaging (New York, NY, United States) and the Michael Wolk Foundation (New York, NY, United States).

REFERENCES

1. Meijboom WB, Meijs MF, Schuijf JD, Cramer MJ, Mollet NR, van Mieghem CA, et al. Diagnostic accuracy of 64-slice computed tomography coronary angiography: a prospective, multicenter, multivendor study. J Am Coll Cardiol 2008;52:2135–44.
2. Miller JM, Rochitte CE, Dewey M, Arbab-Zadeh A, Niinuma H, Gottlieb I, et al. Diagnostic performance of coronary angiography by 64-row CT. N Engl J Med 2008;359:2324–36.
3. Budoff MJ, Dowe D, Jollis JG, Gitter M, Sutherland J, Halamert E, et al. Diagnostic performance of 64-multidetector row coronary computed tomographic angiography for evaluation of coronary artery stenosis in individuals without known coronary artery disease: results from the prospective multicenter ACCURACY (Assessment by Coronary Computed Tomographic Angiography of Individuals Undergoing Invasive Coronary Angiography) trial. J Am Coll Cardiol 2008;52:1724–32.
4. Douglas PS, Hoffmann U, Patel MR, Mark DB, Al-Khalidi HR, Cavanaugh B, et al. Outcomes of anatomical versus functional testing for coronary artery disease. N Engl J Med 2015;372:1291–300.
5. Meijboom WB, van Mieghem CA, Mollet NR, Pugliese F, Weustink AC, van Pelt N, et al. 64-slice computed tomography coronary angiography in patients with high, intermediate, or low pretest probability of significant coronary artery disease. J Am Coll Cardiol 2007;50:1469–75.
6. Taylor AJ, Cerqueira M, Hodgson JM, Mark D, Min J, O'Gara P, et al. ACCF/SCCT/ACR/AHA/ASE/ASNC/NASCI/SCAI/SCMR 2010 appropriate use criteria for cardiac computed tomography. A report of the American College of Cardiology Foundation Appropriate Use Criteria Task Force, the Society of Cardiovascular Computed Tomography, the American College of Radiology, the American Heart Association, the American Society of Echocardiography, the American Society of Nuclear Cardiology, the North American Society for Cardiovascular Imaging, the Society for Cardiovascular Angiography and Interventions, and the Society for Cardiovascular Magnetic Resonance. J Am Coll Cardiol 2010;56:1864–94.

7. Meijboom WB, Van Mieghem CA, van Pelt N, Weustink A, Pugliese F, Mollet NR, et al. Comprehensive assessment of coronary artery stenoses: computed tomography coronary angiography versus conventional coronary angiography and correlation with fractional flow reserve in patients with stable angina. J Am Coll Cardiol 2008;52:636–43.
8. Maurovich-Horvat, P. Schlett CL, Alkadhi H, Nakano M, Otsuka F, Stolzmann P, et al. The napkin-ring sign indicates advanced atherosclerotic lesions in coronary CT angiography. JACC Cardiovasc Imaging 2012;5:1243–52.
9. Leber AW, Becker A, Knez A, von Ziegler F, Sirol M, Nikolaou K, et al. Accuracy of 64-slice computed tomography to classify and quantify plaque volumes in the proximal coronary system: a comparative study using intravascular ultrasound. J Am Coll Cardiol 2006;47:672–7.
10. Pundziute G, Schuijf JD, Jukema JW, Decramer I, Sarno G, Vanhoenacker PK, et al. Head-to-head comparison of coronary plaque evaluation between multislice computed tomography and intravascular ultrasound radiofrequency data analysis. JACC Cardiovasc Interv 2008;1:176–82.
11. Virmani R, Kolodgie FD, Burke AP, Farb A, Schwartz SM. Lessons from sudden coronary death: a comprehensive morphological classification scheme for atherosclerotic lesions. Arterioscler Thromb Vasc Biol 2000;20:1262–75.
12. Schroeder S, Kopp AF, Baumbach A, Meisner C, Kuettner A, Georg C, et al. Noninvasive detection and evaluation of atherosclerotic coronary plaques with multislice computed tomography. J Am Coll Cardiol 2001;37:1430–5.
13. Leber AW, Knez A, Becker A, Becker C, von Ziegler F, Nikolaou K, et al. Accuracy of multidetector spiral computed tomography in identifying and differentiating the composition of coronary atherosclerotic plaques: a comparative study with intracoronary ultrasound. J Am Coll Cardiol 2004;43:1241–7.
14. Hoffmann U, Moselewski F, Nieman K, Jang IK, Ferencik M, Rahman AM, et al. Noninvasive assessment of plaque morphology and composition in culprit and stable lesions in acute coronary syndrome and stable lesions in stable angina by multidetector computed tomography. J Am Coll Cardiol 2006;47:1655–62.
15. Choi BJ, Kang DK, Tahk SJ, Choi SY, Yoon MH, Lim HS, et al. Comparison of 64-slice multidetector computed tomography with spectral analysis of intravascular ultrasound backscatter signals for characterizations of noncalcified coronary arterial plaques. Am J Cardiol 2008;102:988–93.
16. Kwan AC, Cater G, Vargas J, Bluemke DA. Beyond coronary stenosis: coronary computed tomographic angiography for the assessment of atherosclerotic plaque burden. Curr Cardiovasc Imaging Rep 2013;6:89–101.
17. Achenbach S, Ropers D, Hoffmann U, MacNeill B, Baum U, Pohle K, et al. Assessment of coronary remodeling in stenotic and nonstenotic coronary atherosclerotic lesions by multidetector spiral computed tomography. J Am Coll Cardiol 2004;43:842–7.
18. Gauss S, Achenbach S, Pflederer T, Schuhback A, Daniel WG, Marwan M. Assessment of coronary artery remodelling by dual-source CT: a head-to-head comparison with intravascular ultrasound. Heart 2011;97:991–7.
19. Kashiwagi M, Tanaka A, Kitabata H, Tsujioka H, Kataiwa H, Komukai K, et al. Feasibility of noninvasive assessment of thin-cap fibroatheroma by multidetector computed tomography. JACC Cardiovasc Imaging 2009;2:1412–9.
20. van Velzen JE, de Graaf FR, de Graaf MA, Schuijf JD, Kroft LJ, de Roos A, et al. Comprehensive assessment of spotty calcifications on computed tomography angiography: comparison to plaque characteristics on intravascular ultrasound with radiofrequency backscatter analysis. J Nucl Cardiol 2011;18:893–903.
21. Maurovich-Horvat P, Ferencik M, Voros S, Merkely B, Hoffmann U. Comprehensive plaque assessment by coronary CT angiography. Nat Rev Cardiol 2014;11:390–402.
22. Motoyama S, Sarai M, Harigaya H, Anno H, Inoue K, Hara T, et al. Computed tomographic angiography characteristics of atherosclerotic plaques subsequently resulting in acute coronary syndrome. J Am Coll Cardiol 2009;54:49–57.
23. Otsuka K, Fukuda S, Tanaka A, Nakanishi K, Taguchi H, Yoshikawa J, et al. Napkin-ring sign on coronary CT angiography for the prediction of acute coronary syndrome. JACC Cardiovascular imaging 2013;6:448–57.
24. Puchner SB, Liu T, Mayrhofer T, Truong QA, Lee H, Fleg JL, et al. High-risk plaque detected on coronary CT angiography predicts acute coronary syndromes independent of significant stenosis in acute chest pain: results from the ROMICAT-II trial. J Am Coll Cardiol 2014;64:684–92.
25. Park HB, Heo R, o Hartaigh B, Cho I, Gransar H, Nakazato R, et al. Atherosclerotic plaque characteristics by CT angiography identify coronary lesions that cause ischemia: a direct comparison to fractional flow reserve. JACC Cardiovasc Imaging 2015;8:1–10.
26. Sun J, Zhang Z, Lu B, Yu W, Yang Y, Zhou Y, et al. Identification and quantification of coronary atherosclerotic plaques: a comparison of 64-MDCT and intravascular ultrasound. AJR Am J Roentgenol 2008;190:748–54.
27. Hur J, Kim YJ, Lee HJ, Nam JE, Choe KO, Seo JS, et al. Quantification and characterization of obstructive coronary plaques using 64-slice computed tomography: a comparison with intravascular ultrasound. J Comput Assist Tomogr 2009;33:186–92.
28. Danad I, Fayad ZA, Willemink MJ, Min JK. New applications of

cardiac computed tomography: dual-energy, spectral, and molecular CT imaging. JACC Cardiovasc Imaging 2015;8:710–23.
29. Lee JH, Han D, Danad I, Hartaigh BO, Lin FY, Min JK. Multimodality imaging in coronary artery disease: focus on computed tomography. J Cardiovasc Ultrasound 2016;24:7–17.
30. Obaid DR, Calvert PA, Gopalan D, Parker RA, West NE, Goddard M, et al. Dual-energy computed tomography imaging to determine atherosclerotic plaque composition: a prospective study with tissue validation. Journal of cardiovascular computed tomography 2014;8:230–7.
31. Pijls NH, De Bruyne B, Peels K, Van Der Voort PH, Bonnier HJ, Bartunek J Koolen JJ, et al. Measurement of fractional flow reserve to assess the functional severity of coronary-artery stenoses. N Engl J Med 1996;334:1703–8.
32. Tonino PA, De Bruyne B, Pijls NH, Siebert U, Ikeno F, van' t Veer M, et al. Fractional flow reserve versus angiography for guiding percutaneous coronary intervention. N Engl J Med 2009;360:213–24.
33. Morris PD, van de Vosse FN, Lawford PV, Hose DR, Gunn JP. "Virtual" (computed) fractional flow reserve: current challenges and limitations. JACC Cardiovasc Interv 2015;8:1009–17.
34. Grunau GL, Min JK, Leipsic J. Modeling of fractional flow reserve based on coronary CT angiography. Curr Cardiol Rep 2013;15:336.
35. Zarins CK, Taylor CA, Min JK. Computed fractional flow reserve (FFTCT) derived from coronary CT angiography. J Cardiovasc Transl Res 2013;6:708–14.
36. Koo BK, Erglis A, Doh JH, Daniels DV, Jegere S, Kim HS, et al. Diagnosis of ischemia-causing coronary stenoses by noninvasive fractional flow reserve computed from coronary computed tomographic angiograms. Results from the prospective multicenter DISCOVER-FLOW (Diagnosis of Ischemia-Causing Stenoses Obtained Via Noninvasive Fractional Flow Reserve) study. J Am Coll Cardiol 2011;58:1989–97.
37. Min JK, Leipsic J, Pencina MJ, Berman DS, Koo BK, van Mieghem C, et al. Diagnostic accuracy of fractional flow reserve from anatomic CT angiography. Jama 2012;308:1237–45.
38. Norgaard BL, Leipsic J, Gaur S, Seneviratne S, Ko BS, Ito H, et al. Diagnostic performance of noninvasive fractional flow reserve derived from coronary computed tomography angiography in suspected coronary artery disease: the NXT trial (Analysis of Coronary Blood Flow Using CT Angiography: Next Steps). J Am Coll Cardiol 2014;63:1145–55.
39. Renker M, Schoepf UJ, Wang R, Meinel FG, Rier JD, Bayer RR II, et al. Comparison of diagnostic value of a novel noninvasive coronary computed tomography angiography method versus standard coronary angiography for assessing fractional flow reserve. Am J Cardiol 2014;114:1303–8.
40. Coenen A, Lubbers MM, Kurata A, Kono A, Dedic A, Chelu RG, et al. Fractional flow reserve computed from noninvasive CT angiography data: diagnostic performance of an on-site clinician-operated computational fluid dynamics algorithm. Radiology 2015;274:674–83.
41. De Geer J, Sandstedt M, Bjorkholm A, Alfredsson J, Janzon M, Engvall J, et al. Software-based on-site estimation of fractional flow reserve using standard coronary CT angiography data. Acta Radiol 2016;57:1186–92.
42. Douglas PS, Pontone G, Hlatky MA, Patel MR, Norgaard BL, Byrne RA, et al. Clinical outcomes of fractional flow reserve by computed tomographic angiography-guided diagnostic strategies vs. usual care in patients with suspected coronary artery disease: the prospective longitudinal trial of FFR(CT): outcome and resource impacts study. Eur Heart J 2015;36:3359–67.
43. Douglas PS, De Bruyne B, Pontone G, Patel MR, Norgaard BL, Byrne RA, et al. 1-Year Outcomes of FFRCT-guided care in patients with suspected coronary disease: The PLATFORM study. J Am Coll Cardiol 2016;68:435–45.
44. Kim K-H, Doh J-H, Koo B-K, Min JK, Erglis A, Yang HM, et al. A novel noninvasive technology for treatment planning using virtual coronary stenting and computed tomography-derived computed fractional flow reserve. JACC Cardiovasc Interv 2014;7:72–8.
45. Rizvi A, Hartaigh BO, Knaapen P, Leipsic J, Shaw LJ, Andreini D, et al. Rationale and design of the CREDENCE trial: computed TomogRaphic evaluation of atherosclerotic DEtermiNants of myocardial IsChEmia. BMC Cardiovasc Disord 2016;16:190.
46. Truong QA, Knaapen P, Pontone G, Andreini D, Leipsic J, Carrascosa P, et al. Rationale and design of the dual-energy computed tomography for ischemia determination compared to "gold standard" non-invasive and invasive techniques (DECIDE-Gold): A multicenter international efficacy diagnostic study of rest-stress dual-energy computed tomography angiography with perfusion. J Nucl Cardiol 2015;22:1031–40.
47. Pontone G, Andreini D, Guaricci AI, Guglielmo M, Mushtaq S, Baggiano A, et al. Rationale and design of the PERFECTION (comparison between stress cardiac computed tomography PERfusion versus Fractional flow rEserve measured by Computed Tomography angiography In the evaluation of suspected cOroNary artery disease) prospective study. J Cardiovasc Comput Tomogr 2016;10:330–4.
48. Sarno G, Decraemer I, Vanhoenacker PK, De Bruyne B, Hamilos M, Cuisset T, et al. On the inappropriateness of noninvasive multidetector computed tomography coronary angiography to trigger coronary revascularization: a comparison with invasive angiography. JACC Cardiovasc Interv 2009;2:550–7.

49. Schuijf JD, Wijns W, Jukema JW, Atsma DE, de Roos A, Lamb HJ, et al. Relationship between noninvasive coronary angiography with multi-slice computed tomography and myocardial perfusion imaging. J Am Coll Cardiol 2006;48:2508–14.
50. Gaemperli O, Schepis T, Koepfli P, Valenta I, Soyka J, Leschka S, et al. Accuracy of 64-slice CT angiography for the detection of functionally relevant coronary stenoses as assessed with myocardial perfusion SPECT. Eur J Nucl Med Mol Imaging 2007;34:1162–71.
51. Pflederer T, Marwan M, Renz A, Bachmann S, Ropers D, Kuettner A, et al. Noninvasive assessment of coronary in-stent restenosis by dual-source computed tomography. Am J Cardiol 2009;103:812–7.
52. Tashakkor AY, Nicolaou S, Leipsic J, Mancini GB. The emerging role of cardiac computed tomography for the assessment of coronary perfusion: a systematic review and meta-analysis. Can J Cardiol 2012;28:413–22.
53. Varga-Szemes A, Meinel FG, De Cecco CN, Fuller SR, Bayer RR, 2nd, Schoepf UJ. CT myocardial perfusion imaging. AJR Am J Roentgenol 2015;204:487–97.
54. Feger S, Rief M, Zimmermann E, Richter F, Roehle R, Dewey M, et al. Patient satisfaction with coronary CT angiography, myocardial CT perfusion, myocardial perfusion MRI, SPECT myocardial perfusion imaging and conventional coronary angiography. Eur Radiol 2015;25:2115–24.
55. Seitun S, Castiglione Morelli M, Budaj I, Boccalini S, Galletto Pregliasco A, Valbusa A, et al. Stress computed tomography myocardial perfusion imaging: a new topic in cardiology. Rev Esp Cardiol (Engl Ed) 2016;69:188-200.
56. Bettencourt N, Rocha J, Ferreira N, Pires-Morais G, Carvalho M, Leite D, et al. Incremental value of an integrated adenosine stress-rest MDCT perfusion protocol for detection of obstructive coronary artery disease. J Cardiovasc Comput Tomogr 2011;5:392–405.
57. Magalhaes TA, Kishi S, George RT, Arbab-Zadeh A, Vavere AL, Cox C, et al. Combined coronary angiography and myocardial perfusion by computed tomography in the identification of flow-limiting stenosis - The CORE320 study: an integrated analysis of CT coronary angiography and myocardial perfusion. J Cardiovasc Comput Tomogr 2015;9:438–45.
58. Pelgrim GJ, Dorrius M, Xie X, den Dekker MA, Schoepf UJ, Henzler T, et al. The dream of a one-stop-shop: meta-analysis on myocardial perfusion CT. Eur J Radiol 2015;84:2411–20.
59. Kitagawa K, George RT, Arbab-Zadeh A, Lima JA, Lardo AC. Characterization and correction of beam-hardening artifacts during dynamic volume CT assessment of myocardial perfusion. Radiology 2010;256:111–8.
60. Carrascosa PM, Cury RC, Deviggiano A, Capunay C, Campisi R, López de Munain M, et al. Comparison of myocardial perfusion evaluation with single versus dual-energy CT and effect of beam-hardening artifacts. Acad Radiol 2015;22:591–9.
61. Techasith T, Cury RC. Stress myocardial CT perfusion: an update and future perspective. JACC Cardiovasc Imaging 2011;4:905–16.
62. Hill KD, Einstein AJ. New approaches to reduce radiation exposure. Trends Cardiovasc Med 2016;26:55–65.
63. Kim SM, Cho YK, Choe YH. Adenosine-stress dynamic myocardial perfusion imaging using 128-slice dual-source CT in patients with normal body mass indices: effect of tube voltage, tube current, and iodine concentration on image quality and radiation dose. Int J Cardiovasc Imaging 2014;30(Suppl 2):95–103.
64. Asferg C, Usinger L, Kristensen TS, Abdulla J. Accuracy of multislice computed tomography for measurement of left ventricular ejection fraction compared with cardiac magnetic resonance imaging and two-dimensional transthoracic echocardiography: a systematic review and meta-analysis. Eur J Radiol 2012;81:e757–62.
65. Sugeng L, Mor-Avi V, Weinert L, Niel J, Ebner C, Steringer-Mascherbauer R, et al. Multimodality comparison of quantitative volumetric analysis of the right ventricle. JACC Cardiovascular imaging 2010;3:10–8.
66. Dillman JR, Hernandez RJ. Role of CT in the evaluation of congenital cardiovascular disease in children. AJR Am J Roentgenol 2009;192:1219–31.
67. Siripornpitak S, Pornkul R, Khowsathit P, Layangool T, Promphan W, Pongpanich B. Cardiac CT angiography in children with congenital heart disease. Eur J Radiol 2013;82:1067–82.
68. Bean MJ, Pannu H, Fishman EK. Three-dimensional computed tomographic imaging of complex congenital cardiovascular abnormalities. J Comput Assist Tomogr 2005;29:721–4.
69. Han BK, Rigsby CK, Hlavacek A, Leipsic J, Nicol ED, Siegel MJ, et al. Computed tomography imaging in patients with congenital heart disease part i: rationale and utility. an expert consensus document of the Society of Cardiovascular Computed Tomography (SCCT): endorsed by the Society of Pediatric Radiology (SPR) and the North American Society of Cardiac Imaging (NASCI). J Cardiovasc Comput Tomogr 2015;9:475–92.
70. Zhang LJ, Zhou CS, Wang Y, Jin Z, Yu W, Zhang Z, et al. Prevalence and types of coronary to pulmonary artery fistula in a Chinese population at dual-source CT coronary angiography. Acta Radiol (Stockholm, Sweden: 1987) 2014;55:1031–9.
71. Shen Q, Pa M, Hu X, Wang J. Role of plain radiography and CT angiography in the evaluation of obstructed total anomalous pulmonary venous connection. Pediatr Radiol 2013;43:827–35.
72. Hu XH, Huang GY, Pa M, Li X, Wu L, Liu F, et al. Multidetector CT

angiography and 3D reconstruction in young children with coarctation of the aorta. Pediatr Cardiol 2008;29:726–31.
73. Meinel FG, Huda W, Schoepf UJ, Rao AG, Cho YJ, Baker GH, et al. Diagnostic accuracy of CT angiography in infants with tetralogy of Fallot with pulmonary atresia and major aortopulmonary collateral arteries. J Cardiovasc Comput Tomogr 2013;7:367–75.
74. Cohen MS, Eidem BW, Cetta F, Fogel MA, Frommelt PC, Ganame J, et al. Multimodality imaging guidelines of patients with transposition of the great arteries: a report from the American Society of Echocardiography developed in collaboration with the Society for Cardiovascular Magnetic Resonance and the Society of Cardiovascular Computed Tomography. J Am Soc Echocardiogr 2016;29:571–621.
75. Leon MB, Smith CR, Mack M, Miller DC, Moses JW, Svensson LG, et al. Transcatheter aortic-valve implantation for aortic stenosis in patients who cannot undergo surgery. N Engl J Med 2010;363:1597–607.
76. Smith CR, Leon MB, Mack MJ, Miller DC, Moses JW, Svensson LG, et al. Transcatheter versus surgical aortic-valve replacement in high-risk patients. N Engl J Med 2011;364:2187–98.
77. Leipsic J, Yang TH, Min JK. Computed tomographic imaging of transcatheter aortic valve replacement for prediction and prevention of procedural complications. Circ Cardiovasc Imaging 2013;6:597–605.
78. Gilard M, Eltchaninoff H, Iung B, Donzeau-Gouge P, Chevreul K, Fajadet J, et al. Registry of transcatheter aortic-valve implantation in high-risk patients. N Engl J Med 2012;366:1705–15.
79. Jilaihawi H, Kashif M, Fontana G, Furugen A, Shiota T, Friede G, et al. Cross-sectional computed tomographic assessment improves accuracy of aortic annular sizing for transcatheter aortic valve replacement and reduces the incidence of paravalvular aortic regurgitation. J Am Coll Cardiol 2012;59:1275–86.
80. Binder RK, Webb JG, Willson AB, Urena M, Hansson NC, Norgaard BL, et al. The impact of integration of a multidetector computed tomography annulus area sizing algorithm on outcomes of transcatheter aortic valve replacement: a prospective, multicenter, controlled trial. J Am Coll Cardiol 2013;62:431–8.
81. Gurvitch R, Webb JG, Yuan R, Johnson M, Hague C, Willson AB, et al. Aortic annulus diameter determination by multidetector computed tomography: reproducibility, applicability, and implications for transcatheter aortic valve implantation. JACC Cardiovasc Interv 2011;4:1235–45.
82. Ribeiro HB, Webb JG, Makkar RR, Cohen MG, Kapadia SR, Kodali S, et al. Predictive factors, management, and clinical outcomes of coronary obstruction following transcatheter aortic valve implantation: insights from a large multicenter registry. J Am Coll Cardiol 2013;62:1552–62.
83. Genereux P, Head SJ, Van Mieghem NM, Kodali S, Kirtane AJ, Xu K, et al. Clinical outcomes after transcatheter aortic valve replacement using valve academic research consortium definitions: a weighted meta-analysis of 3,519 patients from 16 studies. J Am Coll Cardiol 2012;59:2317–26.
84. Barbanti M, Yang TH, Rodes Cabau J, Tamburino C, Wood DA, Jilaihawi H, et al. Anatomical and procedural features associated with aortic root rupture during balloon-expandable transcatheter aortic valve replacement. Circulation 2013;128:244–53.
85. Hansson NC, Norgaard BL, Barbanti M, Nielsen NE, Yang TH, Tamburino C, et al. The impact of calcium volume and distribution in aortic root injury related to balloon-expandable transcatheter aortic valve replacement. J Cardiovasc Comput Tomogr 2015;9:382–92.
86. Lacomis JM, Wigginton W, Fuhrman C, Schwartzman D, Armfield DR, Pealer KM. Multi-detector row CT of the left atrium and pulmonary veins before radio-frequency catheter ablation for atrial fibrillation. Radiographics 2003;23 Spec No:S35–48; discussion S48–50.
87. Malchano ZJ, Neuzil P, Cury RC, Holmvang G, Weichet J, Schmidt EJ, et al. Integration of cardiac CT/MR imaging with three-dimensional electroanatomical mapping to guide catheter manipulation in the left atrium: implications for catheter ablation of atrial fibrillation. J Cardiovasc Electrophysiol 2006;17:1221–9.
88. Romero J, Husain SA, Kelesidis I, Sanz J, Medina HM, Garcia MJ. Detection of left atrial appendage thrombus by cardiac computed tomography in patients with atrial fibrillation: a meta-analysis. Circ Cardiovasc Imaging 2013;6:185–94.
89. Bilchick KC, Mealor A, Gonzalez J, Norton P, Zhuo D, Mason P, et al. Effectiveness of integrating delayed computed tomography angiography imaging for left atrial appendage thrombus exclusion into the care of patients undergoing ablation of atrial fibrillation. Heart rhythm 2016;13:12–9.
90. Blanke P, Dvir D, Cheung A, Levine RA, Thompson C, Webb JG, et al. Mitral annular evaluation with CT in the context of transcatheter mitral valve replacement. JACC Cardiovascular Imaging 2015;8:612–5.
91. Giannopoulos AA, Mitsouras D, Yoo SJ, Liu PP, Chatzizisis YS, Rybicki FJ. Applications of 3D printing in cardiovascular diseases. Nat Rev Cardiol 2016;13:701–18.